Enthalpy Relaxation in Polymeric Glasses

ALEKSEY D. DROZDOV

Institute for Industrial Mathematics
4 Hanachtom Street
Beersheba 84311, Israel

Constitutive equations are derived for enthalpy recovery in a glassy polymer after quench from above the glass transition temperature T_g to a temperature T in the sub-T_g region. The model is based on the trapping concept, which treats a disordered medium as an ensemble of cooperatively rearranging regions (CRR) hopping in potential wells as they are thermally activated. Rearrangement occurs when a CRR reaches some liquid-like energy level in a hop. The rate of hops is described by the theory of thermally activated processes, whereas the probability to change trap in a hop is determined by the difference between the current and equilibrium concentrations of cages. A nonlinear parabolic equation is developed for the distribution of traps. This equation is used to describe entropy recovery in amorphous and semicrystalline polymers. Fair agreement is demonstrated between experimental data for poly(ether imide), poly(ethylene terephthalate) and polystyrene and results of numerical simulation. Some phenomenological relations are suggested to predict the effect of temperature, molar mass and degree of crystallinity on material parameters.

INTRODUCTION

This study is concerned with the kinetics of enthalpy recovery in amorphous glassy polymers. Structural relaxation (physical aging) in polymers has attracted substantial attention in the past three decades, see monographs (1–5) and review articles (6–9). This interest may be explained by the fact that changes in the internal structure of polymers strongly affect their physical and mechanical properties. In the past decade, slow dynamics in out-of-equilibrium disordered media (spin glasses, supercooled liquids, metallic glasses, orientational glasses, etc.) has become the focus of attention in physics of condensed matter, see recent reviews (10–17).

Structural relaxation in polymers is conventionally studied in "quench-and-wait" experiments, where a specimen equilibrated at some temperature T_0 above the glass transition temperature T_g is quenched to a temperature $T < T_g$ and is annealed at the fixed temperature T,

$$T(t) = T_0 \quad (T < 0), \quad T(t) = T \quad (T > 0). \qquad (1)$$

It is evidenced as the effect of the waiting time t_e (the time elapsed after quench before the beginning of a test) on physical properties of the specimen. The present work focuses on one-step thermal programs, *Eq 1*, for which a wealth of experimental data is available. It is worth noting, however, that this protocol, *Eq 1*, does not exhibit all peculiarities of the aging process revealed in tests with more complicated thermal programs (18, 19).

A number of molecular theories may be mentioned for structural relaxation in amorphous media. The most widely used concepts are the free volume model (20), the theory of cooperative relaxation (21), the coupling concept (22) and the mode-coupling theory (10). Surveys of constitutive relations for the kinetics of structural relaxation in supercooled liquids may be found in the literature (9, 12–15). Despite significant successes in predicting the behavior of glass-forming liquids, it is conventionally presumed that even the mode-coupling theory (the most advanced among molecular models) fails to adequately describe slowing down in the response of amorphous polymers below the glass transition temperature (23). As a reason for this conclusion, the neglect of cooperativity in the molecular reorientation may be mention which plays the key role in kinetic phenomena in the sub-T_g region.

The objective of this study is to derive constitutive equations for enthalpy relaxation that combine the theory of cooperative relaxation in a version of the model of traps (23–27) with the concept of diffusion in configurational space (28–31). An amorphous polymer is treated as an ensemble of mutually independent cooperatively rearranged regions (CRR) (21). A CRR is

thought of as a globule consisting of scores of strands of long chains (26) that rearrange simultaneously by reorientation of chains caused by large-angle rotations of neighboring strands (23). The characteristic length of a relaxing region in the vicinity of the glass transition temperature amounts to several nanometers (32).

In the phase space, a CRR is treated as a point trapped in its potential well. Cages in the phase space are separated by energy barriers whose heights strongly depend on temperature T. Above the glass transition temperature T_g, the average height of barriers is less than the energy of thermal fluctuation, which implies that CRRs easily change their cages (31). Below T_g, the average height of barriers exceeds the energy of thermal fluctuations, which slows down structural relaxation and results in ergodicity breaking (33). Introducing several hypotheses regarding the kinetics of hops from one potential well to another in the sub-T_g region, we derive a nonlinear parabolic equation for the distribution of CRRs trapped in cages with various potential energies and apply this equation to the analysis of enthalpy recovery in amorphous and semicrystalline polymers. The study focuses on the effects of aging temperature, molar mass and level of crystallinity on adjustable parameters in the constitutive relations.

ENTHALPY RELAXATION

An amorphous polymer is treated as an ensemble of cooperatively rearranged regions. In the phase space, any CRR is modeled as a point located at the bottom level of its potential well. At random times, CRRs hop to higher energy levels as they are thermally agitated. With reference to the transition-state theory (34), we assume that some liquid-like (reference) state exists on the energy landscape. The energy of a potential well is characterized by its depth, w, with respect to the reference energy level. It is assumed that $w > 0$ for any cage and $w = 0$ for the liquid-like energy level.

Denote by $q(\omega)d\omega$ the probability for a CRR to reach (in a hop) the energy level that exceeds the bottom level of its potential well by some value, ω', belonging to the interval $[\omega, \omega + d\omega]$. Referring to the extreme-value statistics (14), we set

$$q(\omega) = A \exp(-A\omega),$$

where A is a material constant. The probability for a CRR in a trap with potential energy w to reach the reference state in an arbitrary hop is given by

$$Q(w) = \int_w^\infty q(\omega)\, d\omega = \exp(-Aw). \tag{2}$$

The average rate of hops in a cage γ is determined by the current temperature T only, $\gamma = \gamma(T)$. The rate of rearrangement R (the ratio of the number of CRRs trapped in cages with energy w and rearranged per unit time to the total number of CRRs located in traps with energy w) equals the product of the rate of hops, γ, by the probability, Q, to reach the reference state in a hop. *Equation 2* results in the Eyring formula (35)

$$R(w) = \gamma \exp(-Aw). \tag{3}$$

Denote by X the (time-uniform) concentration of traps per unit mass, and by $p(t, w)$ the distribution function for CRRs trapped in potential wells with energy w. The number of relaxing regions (per unit mass) located in cages with energies belonging to the interval $[w, w + dw]$ and rearranged during the interval of time $[t, t + dt]$ reads

$$X R(w)\, p(t, w)\, dw dt.$$

Unlike previous studies (28–30), we assume that not all relaxing regions change their traps when they reach the reference state and denote by $F(t, w)$ the ratio of the number of CRRs returning to their traps after rearrangement to the number of those reaching the reference state. The number of relaxing regions leaving their cages (with the energy located within the interval $[w, w + dw]$) per unit mass and unit time is given by

$$X[1 - F(t, w)]\, R(w)\, p(t, w)\, dw.$$

We model a relaxing region as a globule (blob) comprised of strands of long chains and assume [in agreement with the shoving model (36)] that some extra space is necessary for a CRR to be rearranged. With reference to (36), the energy w is thought of as a work spent to shove aside the surrounding medium. When the energy of a thermal fluctuation exceeds this work, the volume of a domain occupied by a relaxing region increases, and some strands change their position (which is treated as a rearrangement event). Afterwards, the surrounding material returns in its initial state, and the globule waits for the next activation act.

We suppose that during the rearrangement event (large-angle rotation of neighboring strands), some temporary crosslinks break and some new crosslinks arise. Here crosslinks are treated in a generalized sense as conventional physical crosslinks, entanglements and van der Waals forces. Creation and annihilation of temporary crosslinks is modeled as a hop of a CRR from a cage with potential energy w to a new cage with some energy w'. Any act of rearrangement is assumed to cause only small changes in the energy w (the energy of crosslinks broken/created during the rearrangement event is small compared to the potential energy w). In the phase space, this hypothesis is tantamount to the assumption that the exchange of CRRs occurs between near neighbors on the energy landscape only, that is between traps with the energy $[w, w + dw]$ and cages with the energy $[w - dw, w]$ and $[w + dw, w + 2dw]$. The balance law for the number of CRRs trapped in cages with the energy belonging to the interval $[w, w + dw]$ reads

$$\frac{\partial p}{\partial t} = -(1 - F)\, Rp + \frac{1}{2}[(1 - F)Rp]_+ + \frac{1}{2}[(1 - F)Rp]_-, \tag{4}$$

where the subscript indices "−" and "+" refer to appropriate quantities for the intervals $[w - dw, w]$ and $[w + dw, w + 2dw]$. Expanding the right-hand side of *Eq 4* into the Taylor series, using *Eq 3* and introducing the notation

$$\Gamma = \frac{1}{2}\gamma dw^2,$$

we arrive at the differential equation for diffusion on the energy landscape

$$\frac{\partial p}{\partial t} = \Gamma\frac{\partial^2}{\partial w^2}[(1 - F)\exp(-Aw)p]. \tag{5}$$

An important advantage of *Eq 5* compared to previous studies (37, 38) is that it does not impose restrictions on the equilibrium density of traps, $p_\infty(w)$, provided that $F = 1$ in thermal equilibrium. In particular, this condition is satisfied provided that

$$F(t, w) = \begin{cases} 1, & p(t, w) \le p_\infty(w), \\ \exp[-\epsilon(p - p_\infty)], & p(t, w) > p_\infty(w), \end{cases} \tag{6}$$

where $\epsilon > 0$ is a material parameter. We adopt the random energy model (39, 40), according to which the initial distribution, $p_0(w)$, and the equilibrium distribution, $p_\infty(w)$, are Gaussian functions

$$p_0(w) = \frac{1}{\sqrt{2\pi}\,\Sigma_0}\exp\left[-\frac{(w - W)^2}{2\Sigma_0^2}\right],$$
$$p_\infty(w) = \frac{1}{\sqrt{2\pi}\,\Sigma_\infty}\exp\left[-\frac{(w - W)^2}{2\Sigma_\infty^2}\right], \tag{7}$$

where W, Σ_0, Σ_∞ are adjustable parameters. These formulas imply that the average equilibrium energies of traps are temperature-independent (the same value W is employed for the initial and equilibrium distribution functions), whereas their variances strongly depend on T. The first assertion is fairly well confirmed by experimental data in mechanical tests for several amorphous polymers (41, 42). The other hypothesis is in agreement with the conventional scenario for the growth in the ruggedness of the energy landscape with a decrease in temperature (14, 27, 43). *Equations 7* describe the distribution of CRRs provided that the inequality

$$\int_{-\infty}^{0} p(t, w)\,dw \ll 1 \tag{8}$$

is fulfilled for any $t \ge 0$. In the sequel, we assume that *Eq 8* holds.

The level of disorder in an ensemble of CRRs is described by the configurational entropy per rearranging region (44),

$$s(t) = -k_B\int_0^\infty p(t, w)\ln p(t, w)\,dw,$$

where k_B is Boltzmann's constant. The configurational enthalpy per CRR, $h(t)$, is expressed in terms of the configurational entropy, $s(t)$, by means of the conventional formula

$$\frac{\partial h}{\partial s} = T.$$

Integration of this equality for a one-step thermal test, *Eq 1*, results in the formula for the configurational enthalpy per unit mass, $H = Xh$. We assume that the relaxing enthalpy per unit mass, $\Delta H(t)$, coincides with changes in the configurational enthalpy, $\Delta H(t) = H(t) - H(0)$. This hypothesis is the main postulate of the coarsening concept, see (14) for details, which asserts that changes in relaxing enthalpy of a disordered medium with time (observed in calorimetric tests) are attributed to changes in the distribution of CRRs with various energies. Simple algebra implies that

$$\Delta H(t) = \Lambda\int_0^\infty [p_0(w)\ln p_0(w) - p(t, w)\ln p(t, w)]\,dw, \tag{9}$$

where

$$\Lambda = k_B T X. \tag{10}$$

Introducing the dimensionless variables $\bar{w} = Aw$ and $\bar{t} = t/t_0$, where t_0 is the characteristic time of aging, and setting $\bar{\Gamma} = A^2\Gamma t_0$, $\bar{W} = AW$ and $\bar{\Sigma}_k = A\Sigma_k$, we arrive at the constitutive model, *Eqs 5, 6, 8, 9*, with adjustable parameters $\bar{W}$, $\bar{\Sigma}_0$, $\bar{\Sigma}_\infty$, $\bar{\Gamma}$, ϵ and Λ. *Equations 5, 8, 9* imply that the quantities $\bar{W}$ and $\bar{\Gamma}$ are interrelated: when one of them is fixed arbitrarily, the other may be chosen to characterize the time scale. For convenience of numerical simulation, we fix $\bar{W}$ and determine $\bar{\Gamma}$ by matching observations. The value $\bar{W} = 2.5$ ensures that *Eq 8* is satisfied with a high level of accuracy and reduces the number of material parameters to five. This number of material constants in governing equations is quite comparable with that used in conventional phenomenological models which employ the stretched exponential function to fit observations (7). As examples, we refer to a model with 4 constants (45–47) that combines the Kohlrausch—Williams—Watts (KWW) formula with the Adam—Gibbs equation (21) for the characteristic time of structural relaxation τ_0 and to a model with 5 constants (48, 49) that employs the KWW equation together with the Narayanaswamy relation for τ_0. A survey of constitutive equations with a higher number of adjustable parameters may be found in (50). An advantage of our model compared to phenomenological approaches is that structural recovery in polymers is described at the molecular level, which provides a unified framework to treat observations in various tests (calorimetric, dilatometric, mechanical, dielectric, etc.).

VALIDATION OF THE MODEL

To verify the constitutive equations, we analyze experimental data for several amorphous and semicrystalline polymers in the sub-T_g region. We begin with observations for amorphous poly(ether imide). For a detailed description of specimens and the experimental procedure, we refer to (51). First, experimental data are fitted at the lowest temperature, T = 190°C. The quantities $\bar{\Sigma}_0$, $\bar{\Sigma}_\infty$, $\bar{\Gamma}$, ϵ and Λ are determined from the condition of the best approximation of observations. Given amounts $\bar{\Sigma}_0$, $\bar{\Sigma}_\infty$, $\bar{\Gamma}$, and ϵ, the constant Λ is found using the least-squares technique. To calculate other adjustable parameters, the steepest-descent algorithm is employed. Afterwards, the parameters $\bar{\Sigma}_0$, ϵ and Λ are fixed, and measurements at higher temperatures are approximated by using only two adjustable parameters, $\bar{\Sigma}_\infty$ and $\bar{\Gamma}$. *Figure 1* demonstrates fair agreement between observations and results of numerical simulation.

The quantities $\bar{\Sigma}_\infty$ and $\bar{\Gamma}$ are plotted in *Figs. 2* and *3* versus the level of super cooling $\Delta T = T_g - T$. These figures show that the dependencies $\bar{\Sigma}_\infty(T)$ and $\bar{\Gamma}(T)$ are correctly approximated by the linear functions

$$\bar{\Sigma}_\infty = a_0 + a_1 \Delta T, \quad \log \bar{\Gamma} = b_0 - b_1 \Delta T, \qquad (11)$$

where a_k and b_k are adjustable parameters. In the vicinity of the glass transition temperature, the apparent activation energy ΔE is calculated as

$$\Delta E = -R \left. \frac{d \ln \bar{\Gamma}}{d(1/T)} \right|_{T=T_g}, \qquad (12)$$

where R is the gas constant. It follows from *Eqs 11, 12* that

$$\Delta E = RT_g^2 \, b_1 \ln 10.$$

This equality together with *Fig. 3* implies that ΔE = 420.5 kJ/mol, which is a typical value of the activation energy for amorphous polymers (52).

We now repeat the approximation procedure using another set of experimental data for poly(ether imide). A detailed description of specimens and the experimental procedure can be found in (53). The relaxing enthalpy is depicted in *Fig. 4* for various temperatures T in the sub-T_g region, whereas the parameters $\bar{\Sigma}_\infty$ and $\bar{\Gamma}$ are plotted in *Figs. 2* and *3* versus the increment of temperature ΔT.

For two kinds of poly(ether imide), the parameters $\bar{\Sigma}_0$ coincide and the quantities ϵ = 0.25 and ϵ = 0.30 are very close to each other. *Figures 2* and *3* reveal that $\bar{\Sigma}_\infty$ and $\bar{\Gamma}$ accept similar values as well, whereas the quantities Λ substantially differ: the concentration of relaxing regions for PEI studied in (53) is about twice that for PEI investigated in (51). Because no data are provided about properties of the specimens, we can only speculate regarding reasons for this difference. As a possible explanation, differences in molar mass and in polydispersity may be mentioned, which dramatically affect the rate of enthalpy recovery (54, 55).

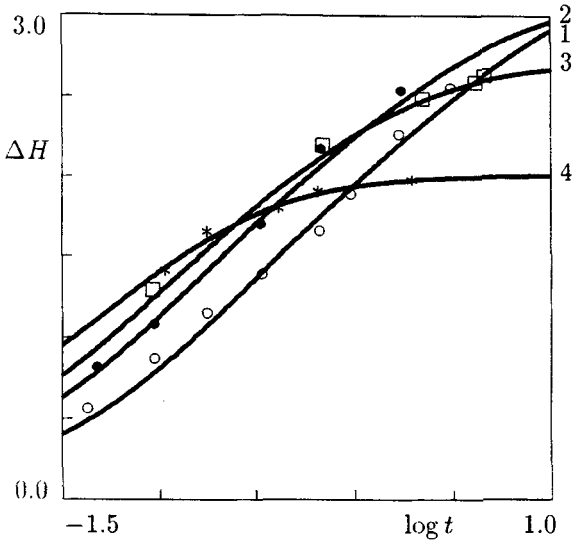

Fig. 1. The relaxation enthalpy ΔH J/g versus time t days for poly(ether imide) (T_g = 213°C) quenched from T_0 = 223 to the test temperature T°C. Symbols: experimental data (51). Solid lines: prediction of the model with $\bar{\Sigma}_0$ = 0.2, ϵ = 0.25 and Λ = 2.1. Curve 1: T = 190; curve 2: T = 193; curve 3: T = 196; curve 4: T = 199.

To analyze the influence of molar mass on adjustable parameters of the model, experimental data are fitted for two kinds of polystyrene. A detailed description of specimens and the experimental procedure is presented in (56). The algorithm for determining adjustable parameters coincides with that for poly(ether imide).

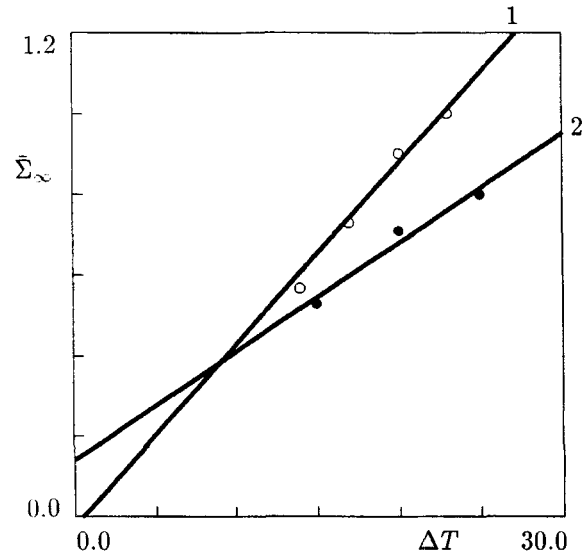

Fig. 2. The parameter $\bar{\Sigma}_\infty$ versus the level of super cooling ΔT°C for poly(ether imide). Symbols—treatment of observations: unfilled circles (51); filled circles (53). Solid lines: approximation of the experimental data by Eq 11. Curve 1: a_0 = − 0.023, a_1 = 0.045; curve 2: a_0 = 0.140, a_1 = 0.027.

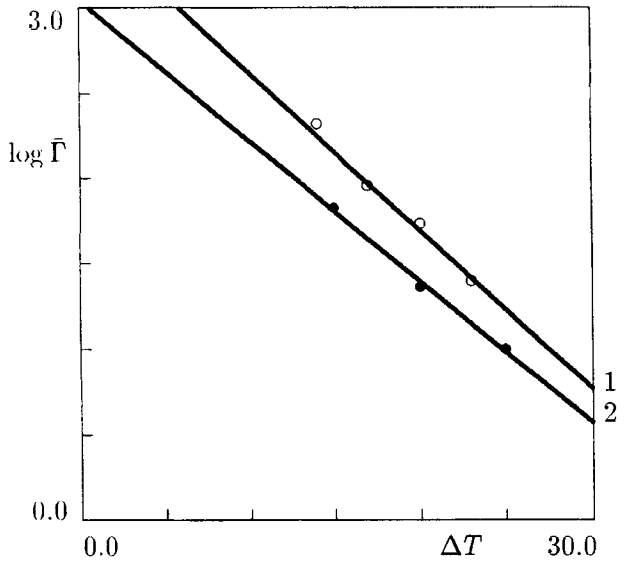

Fig. 3. The parameter $\bar{\Gamma}$ days^{-1} versus the level of super cooling ΔT°C for poly(ether imide). Symbols—treatment of observations: unfilled circles (51); filled circles (53). Solid lines: approximation of the experimental data by Eq 11. Curve 1: $b_0 = 3.549$, $b_1 = 0.093$; curve 2: $b_0 = 3.048$, $b_1 = 0.083$.

Figures 5 and *6* demonstrate fair agreement between observations and results of numerical simulation. The temperature-dependent parameters $\bar{\Sigma}_\infty$ and $\bar{\Gamma}$ are depicted in *Figs. 7* and *8*, which show that *Eq 11* correctly predicts experimental data in the vicinity of the glass transition temperature.

According to *Fig. 7*, an increase in the molar mass (from 0.37×10^5 g/mol for PS37k to 2.67×10^5 g/mol for PS267k when polydispersity remains practically constant) results in a decrease in Σ_∞. The rate of structural relaxation $\bar{\Gamma}$ grows with molar mass. The parameters $\bar{\Sigma}_0$ and Λ are rather close for two kinds of polystyrene, which means that they are weakly affected by molar mass. The coefficient ϵ decreases with the growth of molar mass (approximately by an order), which implies that an increase in molar mass leads to a decrease in the rate of structural relaxation.

Figures 2 and *7* imply that the standard deviation $\bar{\Sigma}_\infty$ decreases with temperature and vanishes in the vicinity of the glass transition temperature. Following (57), the critical temperature T_{cr} may be defined as a temperature at which $\bar{\Sigma}_\infty = 0$ and the energy landscape becomes homogeneous. This temperature may be associated with the critical temperature in the mode-coupling theory for glass transition (10, 13, 16). The maximal critical temperature equals $T_{cr} = T_g + 5.2$ for poly(ether imide) and $T_{cr} = T_g + 15.0$°C for polystyrene. These values are rather close to $T_{cr} = T_g + 8.8$ and $T_{cr} = T_g + 9.4$°C found for polycarbonate and poly(vinyl acetate), respectively, using experimental data in mechanical tests (57).

Calculations of the apparent activation energies ΔE for two kinds of polystyrene implies that $\Delta E = 125.2$ kJ/mol for PS37k and $\Delta E = 241.9$ kJ/mol for PS267k. Both values of ΔE are typical of amorphous glassy polymers. An increase in molar mass leads to the growth of the activation energy, which is in agreement with the concept of cooperative rearrangement in glassy polymers (21).

The model, *Eqs 5*, *6*, *8*, *9*, may be applied to the analysis of structural recovery in amorphous, as well as in semicrystalline polymers. As a possible basis for

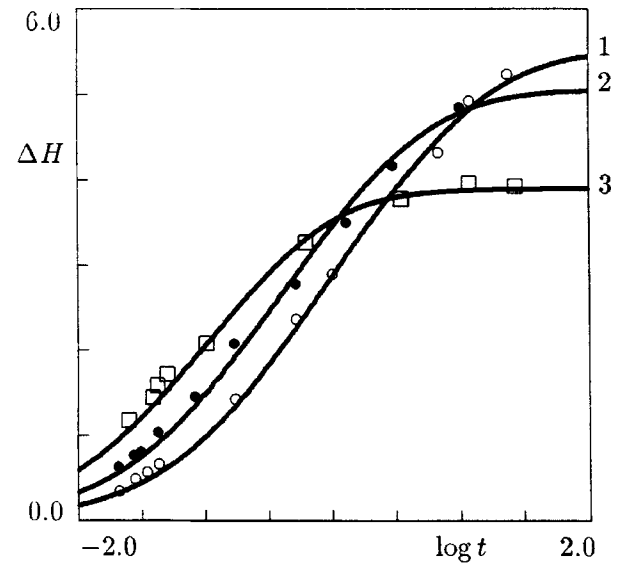

Fig. 4. The relaxing enthalpy ΔH J/g versus time t days for poly(ether imide) (T_g = 215°C) quenched from T_0 = 225 to the test temperature T°C. Symbols: experimental data (53). Solid lines: prediction of the model with $\bar{\Sigma}_0 = 0.2$, $\epsilon = 0.3$ and $\Lambda = 4.0$. Curve 1: T = 190; curve 2: T = 195; curve 3: T = 200.

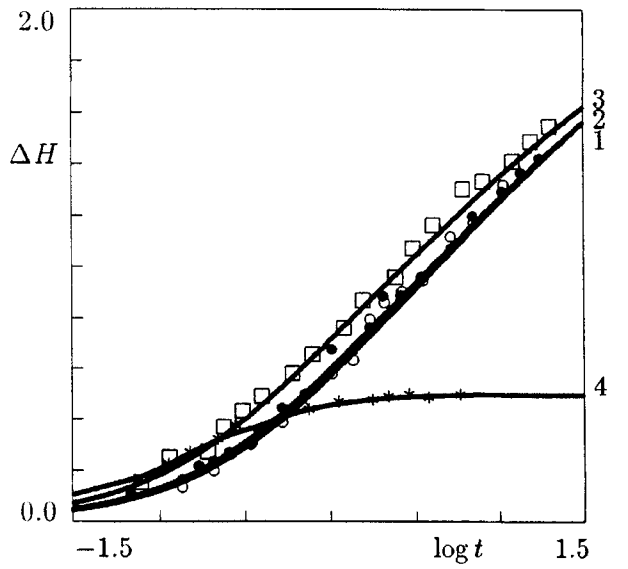

Fig. 5. The relaxing enthalpy ΔH J/g versus time t h for polystyrene PS37k (T_g = 100°C) quenched from T_0 = 150 to the test temperature T°C. Symbols: experimental data (56). Solid lines: prediction of the model with $\bar{\Sigma}_0 = 0.1$, $\epsilon = 1.0$ and $\Lambda = 0.92$. Curve 1: T = 80.0; curve 2: T = 85.0; curve 3: T = 90.0; curve 4: T = 95.0.

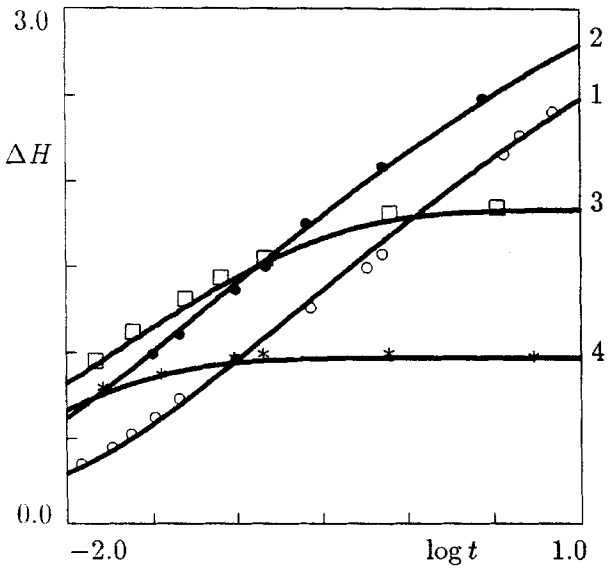

Fig. 6. The relaxing enthalpy ΔH J/g versus time t days for polystyrene PS267k (T_g = 103.6°C) quenched from T_0 = 150 to the test temperature T°C. Symbols: experimental data (56). Solid lines: prediction of the model with $\bar{\Sigma}_0$ = 0.08, ϵ = 0.1 and Λ = 1.2. Curve 1: T = 81.9; curve 2: T = 86.9; curve 3: T = 91.9; curve 4: T = 96.9.

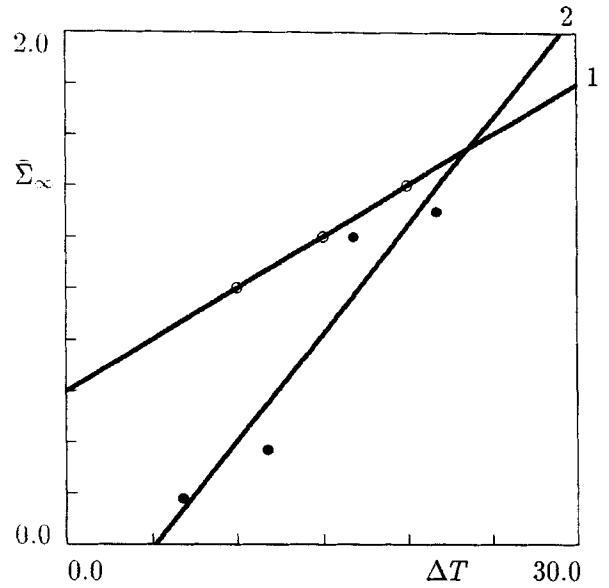

Fig. 7. The parameter $\bar{\Sigma}_\infty$ versus the level of super cooling ΔT°C for polystyrene. Symbols—treatment of observations: unfilled circles: PS37k (56); filled circles: PS267k (56). Solid lines: approximation of the experimental data by Eq 11. Curve 1: a_0 = 0.600, a_1 = 0.040; curve 2: a_0 = −0.436, a_1 = 0.084.

this assertion, we note that physical aging is observed in an amorphous phase of a semicrystalline material only, which implies that the presence of crystalline lamellae may be neglected (at least, as a first approximation). It is conventionally assumed that two kinds of amorphous regions coexist in a semicrystalline polymer: weakly restricted interspherulitic domains and strongly constrained intraspherulitic domains (58, 59). This picture evokes the question which parameters in the constitutive equations and in what way are affected by changes in the degree crystallinity. Attempting to answer this question, we match experimental data for enthalpy relaxation in several semicrystalline polymers where the level of crystallinity is changed in different ways.

We begin with observations for miscible blends of syndiotactic (sPS) and atactic (aPS) polystyrenes with various ratios *f* of their weights. For a description of samples and the experimental procedure, see (60). To match experimental data, we employ the same algorithm, as has been exposed for poly(ether imide) and polystyrene. The quantities $\bar{\Sigma}_0$ and ϵ are determined by fitting data for sPS (*f* = 100/0). In matching observations for other values of *f*, these parameters are assumed to be fixed.

Figure 9 demonstrates excellent agreement between experimental data and results of numerical simulation. The value $\bar{\Sigma}_0$ = 0.12 found by fitting data for polystyrene blends is close to the values $\bar{\Sigma}_0$ = 0.10 for PS37k and $\bar{\Sigma}_0$ = 0.08 for PS267k. Taking into account that the molar mass of the sPS/aPS blends (60) exceeds that for polystyrenes (56), we conclude that $\bar{\Sigma}_0$ is independent of molar mass. The value ϵ = 0.1 found by fitting experimental data for the polystyrene blends coincides with that determined by matching observations for PS267k.

Experimental data for various values of *f* cannot be correctly fitted under the assumption that the parameter Λ remains constant. Adjustable parameters $\bar{\Sigma}_\infty$,

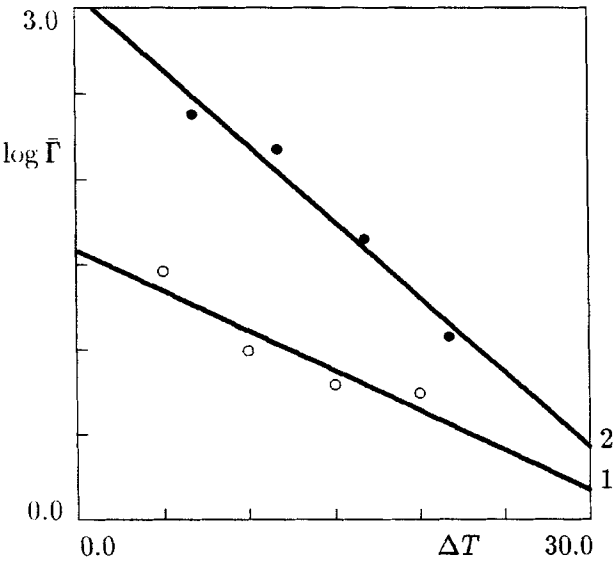

Fig. 8. The parameter $\bar{\Gamma}$ day^{-1} versus the level of super cooling ΔT°C for polystyrene. Symbols—treatment of observations: unfilled circles PS37k (56); filled circles: PS267 (56). Solid lines: approximation of the experimental data by Eq 11. Curve 1: b_0 = 1.585, b_1 = 0.047; curve 2: b_0 = 3.088, b_1 = 0.089.

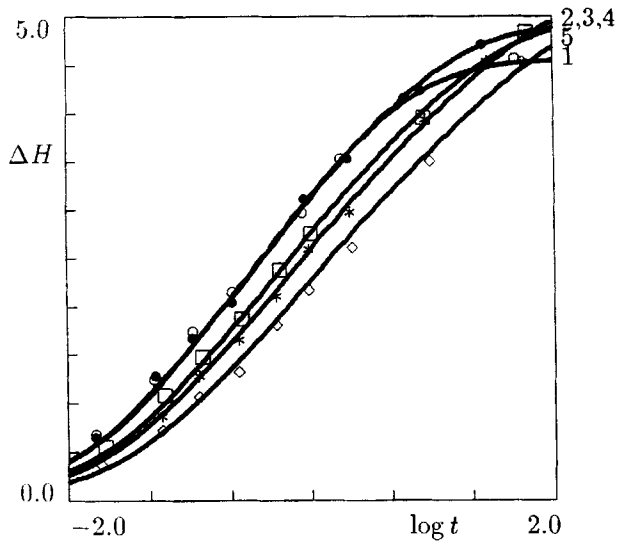

Fig. 9. The relaxing enthalpy ΔH J/g versus time t days for a blend of syndiotactic and atactic polystyrene quenched from T_0 = 300 to T = 80°C. Symbols: experimental data (60). Solid lines: prediction of the model with $\bar{\Sigma}_0$ = 0.12 and ϵ = 0.1. Curve 1: f = 100/0; curve 2: f = 70/30; curve 3: f = 50/50; curve 4: f = 30/70; curve 5: f = 0/100.

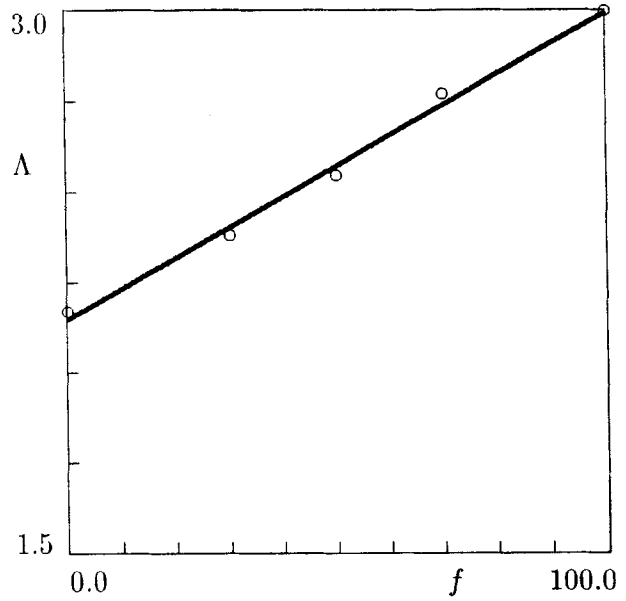

Fig. 11. The parameter Λ J/g versus the sPS/aPS ratio f percent. Circles: treatment of observations (60). Solid line: approximation of the experimental data by Eq 13 with C_0 = 2.148 and C_1 = 0.0084.

$\bar{\Gamma}$ and Λ are plotted versus *f* in *Figs. 10* and *11*. These dependencies may be pretty well approximated by the linear functions

$$\bar{\Sigma}_\infty = A_0 - A_1 f, \quad \bar{\Gamma} = B_0 + B_1 f, \quad \Lambda = C_0 + C_1 f, \quad (13)$$

where A_k, B_k and C_k are positive constants.

Equations 13 imply that the parameter Λ linearly increases with *f*. Because Λ is proportional to the number of CRRs per unit mass, and the sPS/aPS ratio *f* is proportional to molar mass, we find that the concentration of CRRs increases with molar mass. This conclusion is in good agreement with data for two kinds of polystyrene (56), which also demonstrate an increase in Λ with molar mass.

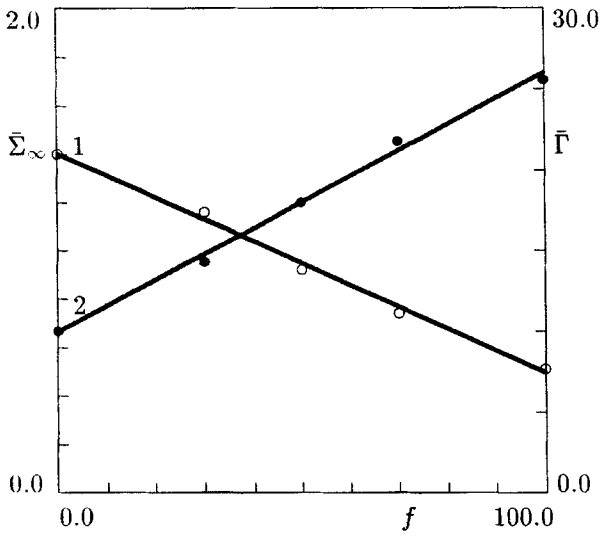

Fig. 10. The parameter $\bar{\Sigma}_\infty$ (curve 1) and the parameter $\bar{\Gamma}$ day^{-1} (curve 2) versus the sPS/aPS ratio f percent. Circles: treatment of observations (60). Solid lines: approximation of the experimental data by Eq 13 with A_0 = 1.403, A_1 = 0.0091 and B_0 = 9.983, B_1 = 0.160.

The last equality in *Eq 13* means that the number of relaxing regions increases with the crystallinity level. At first glance, this conclusion seems paradoxical, because an increase in the degree of crystallinity results in a decrease in the total mass of amorphous regions (where structural relaxation takes place). To resolve this (apparent) contradiction, we recall that volumes of CRRs are proportional to their energies in amorphous polymers only. On the contrary, no one-to-one correspondence may be found between these quantities in semicrystalline polymers: intraspherulitic CRRs are quite small compared to interspherulitic regions (because they are confined to tiny "holes" in crystallites), whereas energies of cages where they are trapped exceed those for interspherulitic domains (since rearrangement of intraspherulitic CRRs is restricted by chains emanated from crystalline domains). This assertion implies that an increase in the degree of crystallinity may result in a growth of the number density of CRRs, in spite of a decrease in the total mass of the amorphous component.

According to *Fig. 10*, $\bar{\Sigma}_\infty$ = 1.40 for amorphous aPS at $T = T_g$ − 23.8°C. Comparing this value with the amounts $\bar{\Sigma}_\infty$ = 1.55 and $\bar{\Sigma}_\infty$ = 1.56 calculated for PS37k and PS267k using data presented in *Fig. 7*, we conclude that the equilibrium standard deviation, $\bar{\Sigma}_\infty$, is practically independent of molar mass.

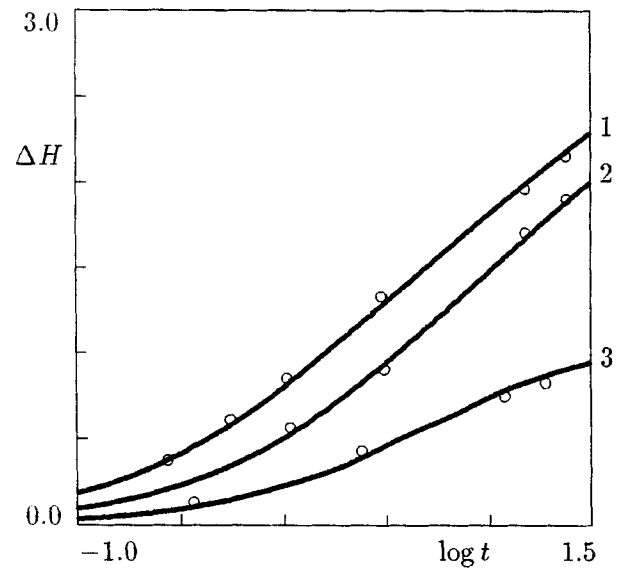

Fig. 12. The relaxing enthalpy ΔH J/g versus time t h for poly(ethylene terephthalate) (T_g = 80°C) quenched from T_0 = 100 to the test temperature T = 65°C. Symbols: experimental data (59). Solid lines: prediction of the model with $\bar{\Sigma}_0$ = 0.2 and ϵ = 0.05. Curve 1: f = 14%; curve 2: f = 21%; curve 3: f = 32%.

It follows from the first two equalities in *Eq 13* that the quantity $\bar{\Sigma}_\infty$ decreases and the parameter $\bar{\Gamma}$ increases with the degree of crystallinity. To check, whether these dependencies remain valid for other semicrystalline polymers, we fit observations for poly(ethylene terephthalate). Physical properties of specimens and the experimental procedure are exposed in (59). Adjustable parameters in the constitutive equations are found by applying the same algorithm as has been described for PEI.

Figure 12 demonstrates fair agreement between experimental data and results of numerical simulation. Matching observations implies that $\bar{\Sigma}_0$ = 0.2 and ϵ = 0.05, which are close to appropriate parameters determined for other polymers. The quantities $\bar{\Sigma}_\infty$, $\bar{\Gamma}$ and Λ are plotted versus the level of crystallinity *f* in *Figs. 13* and *14*. Comparing *Figs. 11* and *14*, we conclude that the effect of the ratio *f* on the concentration of CRRs, Λ, is similar for PS blends and for PET (a linear increase with *f*). *Figures 10* and *13* demonstrate that the standard deviation, $\bar{\Sigma}_\infty$, monotonically decreases with *f*, which means that the homogeneity of the energy landscape of a semicrystalline polymer increases with the growth of the degree of crystallinity. This fact may be explained by the difference between physical properties of intraspherulitic and interspherulitic domains, because the energy landscape for intraspherulitic CRRs is essentially less rugged than that for interspherulitic ones (intraspherulitic regions are confined to tiny "holes" or "layers" within spherulites and are strongly linked to their environment, which implies that the distribution of energies of potential wells where they are trapped should be rather narrow).

Figure 13 reveals that the parameter $\bar{\Sigma}_\infty$ vanishes at f_{cr} = 39%. This implies that some critical level of crystallinity exists above which entropy relaxation disappears. It is worth noting that the parameter $\bar{\Gamma}$ (which is responsible for the rate of structural relaxation) vanishes at the same degree of crystallinity.

A decrease in the relaxing entropy with an increase in the level of crystallinity (qualitatively similar to that depicted in *Fig. 13*) has been already demonstrated in (61) on hot-drawn poly(ethylene terephthalate) at large strains (up to 400%). However, the effects of molecular orientation and the degree of crystallinity (which simultaneously increase at stretching of a specimen) have not been distinguished. The fact that both phenomena dramatically affect the aging process has been discussed in (62).

No detailed explanation may be presented why the function $\bar{\Gamma}(f)$ increases for polystyrene blends and decreases for poly(ethylene terephthalate). As a possible reason for this difference, we would mention the dilution effect in miscible blends, which slows down the crystallization kinetics (60) and prevents disappearance of interspherulitic domains.

CONCLUSIONS

Constitutive equations have been derived for enthalpy relaxation in glassy polymers after thermal jumps. The model is based on the trapping concept which treats a disordered medium as an ensemble of CRRs rearranged at random times as they are thermally activated. Adjustable parameters are found by fitting experimental data for several amorphous and semicrystalline polymers. The following conclusions are drawn:

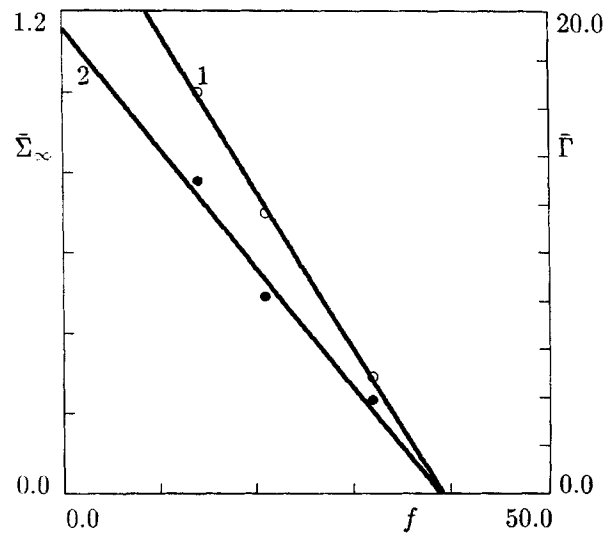

Fig. 13. The parameter $\bar{\Sigma}_\infty$ (curve 1) and the parameter $\bar{\Gamma}$ h^{-1} (curve 2) versus the level of crystallinity f percent for poly(ethylene terephthalate). Circles: treatment of observations (59). Solid lines: approximation of the experimental data by Eq 13 with A_0 = 1.540, A_1 = 0.039 and B_0 = 19.278, B_1 = 0.495.

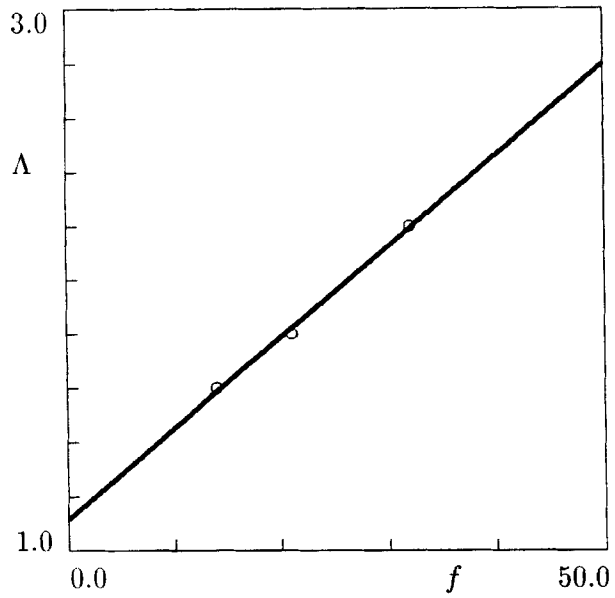

Fig. 14. The parameter Λ J/g versus the level of crystallinity f percent for poly(ethylene terephthalate). Circles: treatment of observations (59). Solid line: approximation of the experimental data by Eq 13 with C_0 = 1.174 and C_1 = 0.0504.

1. The model correctly describes the kinetics of structural relaxation in the sub-T_g region.
2. For amorphous polymers the model predicts the existence of a critical temperature, T_{cr}, at which the energy landscape becomes homogeneous. The location of the critical point is in fair agreement with conclusions of the mode-coupling theory and with previous data obtained by fitting observations in mechanical tests.
3. For semicrystalline polymers the model predicts the existence of a critical degree of crystallinity, f_{cr}, at which the energy landscape becomes homogeneous. Our conjecture is that the presence of this critical point may be explained by the difference between a (homogeneous) energy landscape of intraspherulitic amorphous layers and an (inhomogeneous) energy landscape of interspherulitic amorphous regions.
4. An increase in the annealing temperature, T, leads to changes in material parameters which correspond to predictions of the theory of thermally activated processes.
5. The quantities $\bar{\Sigma}_0$ and $\bar{\Sigma}_\infty$ which determine equilibrium probability densities of traps are practically independent of molar mass.
6. An increase in the level of crystallinity for semicrystalline polymers leads to the growth of the concentration of CRRs and to a decrease in the ruggedness of the energy landscape.
7. The dimensionless parameter ϵ is of the order of unity (about 0.1 for most polymers studied in this work). This means that relaxing regions not necessarily leave their traps when the concentration of CRRs with a given energy is higher than that in thermal equilibrium. The parameter ϵ (responsible for the kinetics of structural relaxation) is practically independent of molar mass and the degree of crystallinity.

ACKNOWLEDGMENT

The work was supported by the Israeli Ministry of Science through grant 1202-1-00.

REFERENCES

1. L. C. E. Struik, *Physical Aging in Amorphous Polymers and Other Materials*, Elsevier, Amsterdam (1978).
2. S. A. Brawer, *Relaxation in Viscous Liquids and Glasses*, Am. Ceram. Soc., Columbus (1985).
3. E.-J. Donth, *Relaxation and Thermodynamics in Polymers: Glass Transition*, Academie-Verlag, Berlin (1992).
4. S. Matsuoka, *Relaxation Phenomena in Polymers*, Hanser-Verlag, Munich (1992).
5. A. D. Drozdov, *Mechanics of Viscoelastic Solids*, Wiley, Chichester (1998).
6. G. B. McKenna, in *Comprehensive Polymer Science*, Vol. 2, p. 311, C. Booth and C. Price, eds., Oxford, Pergamon Press (1989).
7. C. T. Moynihan, S. N. Crichton, and S. M. Opalka, *J. Non-Cryst. Solids*, **131–133**, 420 (1991).
8. I. M. Hodge, *J. Non-Cryst. Solids*, **169**, 211 (1994).
9. M. D. Ediger, C. A. Angell, and S. R. Nagel, *J. Phys. Chem.*, **100**, 13200 (1996).
10. W. Götze and L. Sjögren, *Rep. Prog. Phys.* **55**, 241 (1992).
11. P. G. Debenedetti, *Metastable Liquids: Concepts and Principles*, Princeton Univ. Press, Princeton N.J. (1996).
12. H. Z. Cummins, G. Li, Y. H. Hwang, G. Q. Shen, W. M. Du, J. Hernandez, and N. J. Tao, *Z. Phys. B*, **103**, 501 (1997).
13. W. Kob, in *Experimental and Theoretical Approaches to Supercooled Liquids: Advances and Novel Applications*, p. 28, J. Fourcas, D. Kivelson, U. Mohanty, and K. Nelson, eds., ACS Books, Washington (1997).
14. J.-P. Bouchaud, L. F. Cugliandolo, J. Kurchan, and M. Mezard, in *Spin Glasses and Random Fields*, p. 161, A. P. Young, ed., World Scientific, Singapore (1998).
15. J.-P. Bouchaud, Preprint cond-mat/9910387.
16. W. Kob, Preprint cond-mat/9911023.
17. J. Hammann, E. Vincent, V. Dupuis, M. Alba, M. Ocio, and J.-P. Bouchaud, Preprint cond-mat/9911269.
18. L. Bellon, S. Ciliberto, and C. Laroche, Preprint cond-mat/9905160.
19. L. Bellon, S. Ciliberto, and C. Laroche, Preprint cond-mat/9906162.
20. M. H. Cohen and G. S. Grest, *Phys. Rev. B*, **20**, 1077 (1979).
21. G. Adam and J. H. Gibbs, *J. Chem. Phys.*, **43**, 139 (1965).
22. R. W. Rendell, K. L. Ngai, G. R. Fong, and J. J. Aklonis, *Macromolecules*, **20**, 1070 (1987).
23. J. C. Dyre, *Phys. Rev. B*, **51**, 12276 (1995).
24. J. P. Bouchaud, *J. Phys. I France*, **2**, 1705 (1992).
25. C. Monthus and J.-P. Bouchaud, *J. Phys. A*, **29**, 3847 (1996).
26. P. Sollich, *Phys. Rev. E*, **58**, 738 (1998).
27. G. Diezemann, U. Mohanty, and I. Oppenheim, *Phys. Rev. E*, **59**, 2067 (1999).
28. R. E. Robertson, *J. Appl. Phys.*, **49**, 5048 (1978).
29. R. E. Robertson, R. Simha, and J. G. Curro, *Macromolecules* **17**, 911 (1984).
30. T. S. Chow, *J. Chem. Phys.*, **79**, 4602 (1983).

31. H. Bassler, *Phys. Rev. Lett.*, **58**, 767 (1987).
32. A. K. Rizos and K. L. Ngai, *Phys. Rev. E*, **59**, 612 (1999).
33. R. G. Palmers, *Adv. Phys.*, **31**, 669 (1982).
34. M. Goldstein, *J. Chem. Phys.*, **51**, 3728 (1969).
35. H. Eyring, *J. Chem. Phys.*, **4**, 283 (1936).
36. J. C. Dyre, *J. Non-Cryst. Solids*, **235–237**, 142 (1998).
37. P. Feltham, *Phys. Stat. Sol.*, **30**, 135 (1968).
38. F. Dobes, *Acta Metall.*, **28**, 377 (1980).
39. B. Derrida, *Phys. Rev. B*, **24**, 2613 (1981).
40. R. Richert and H. Bassler, *J. Phys.: Condens. Matter*, **2**, 2273 (1990).
41. A. D. Drozdov, *Comput. Mater. Sci.*, **15**, 422 (1999).
42. A. D. Drozdov, *Modelling Simul. Mater. Sci. Eng.*, **7**, 1045 (1999).
43. C. M. Roland, P. G. Santangelo, and K. L. Ngai, *J. Chem. Phys.*, **111**, 5593 (1999).
44. I. Avramov and A. Milchev, *J. Non-Cryst. Solids*, **104**, 253 (1988).
45. J. L. Gomez Ribelles and M. Monleon Pradas, *Macromolecules*, **28**, 5867, 5878 (1995).
46. A. Brunacci, J. M. G. Cowie, R. Ferguson, J. L. Gomez, Ribelles, and A. Vidaurre Garayo, *Macromolecules*, **29**, 7976 (1996).
47. J. M. G. Cowie, S. Harris, J. L. Gomez Ribelles, J. M. Meseguer, F. Romero, and C. Torregrosa, *Macromolecules*, **32**, 4430 (1999).
48. I. M. Hodge and A. R. Berens, *Macromolecules*, **15**, 762 (1982).
49. J. M. Hutchinson, S. Smith, B. Horne, and G. M. Gourlay, *Macromolecules*, **32**, 5046 (1999).
50. I. M. Hodge, *Macromolecules*, **20**, 2897 (1987).
51. H. Yoshida, *Thermochim. Acta*, **266**, 119 (1995).
52. J. D. Ferry, *Viscoelastic Properties of Polymers*, Wiley, New York (1980).
53. E. M. Woo and S.-M. Kuo, *Polym. Eng. Sci.*, **37**, 173 (1997).
54. A. S. Marshall and S. E. B. Petrie, *J. Appl. Phys.*, **46**, 4223 (1975).
55. H. Yoshida and Y. Kobayashi, *Polym. Eng. Sci.*, **23**, 907 (1983).
56. A. Brunacci, J. M. G. Cowie, R. Ferguson, and I. J. McEwen, *Polymer*, **38**, 865, 3263 (1997).
57. A. D. Drozdov, *Europhys. Lett.*, **49**, 569 (2000).
58. K. H. Illers and H. Breuer, *J. Coll. Sci.*, **18**, 1 (1963).
59. J. A. Diego, J. C. Canadas, M. Mudarra, and J. Belana, *Polymer*, **40**, 5355 (1999).
60. B. K. Hong, W. H. Jo, and J. Kim, *Polymer*, **39**, 3753 (1998).
61. S. Mukherjee and S. A. Jabarin, *Polym. Eng. Sci.*, **35**, 1145 (1995).
62. M. D. Shelby and G. L. Wilkes, *Polymer*, **39**, 6767 (1998).